encit 2020

ABCM Associação Brasileira de Engenharia e Ciências Mecânicas

18th Brazilian Congress of Thermal Sciences and Engineering
November 16–20, 2020 (online)

ENC-2020-0068
COMPARATIVE STUDY OF A DIRECTED EXPANSION SOLAR ASSISTED HEAT PUMP USING CAPILLARY TUBES AND THERMOSTATIC EXPANSION VALVE

André Gonçalves de Oliveira
Hélio Augusto Goulart Diniz
Federal University of Minas Gerais (UFMG), Post-Graduate Program in Mechanical Engineering, Av. Antonio Carlos, 6627, Belo Horizonte - MG, 31270-901, Brazil
andreqix@hotmail.com, helioufmg@gmail.com

Willian Moreira Duarte
Federal University of Minas Gerais (UFMG), Post-Graduate Program in Mechanical Engineering, Belo Horizonte - MG, Brazil
University Center of Belo Horizonte (UniBH), Department of Mechanical Engineering, Av. Prof. Mário Werneck, 1685, Estoril, 30575-180, Belo Horizonte (MG), Brazil
willianmoreiraduarte@gmail.com

Luiz Machado
Raphael Nunes Oliveira
Federal University of Minas Gerais (UFMG), Post-Graduate Program in Mechanical Engineering, Av. Antonio Carlos, 6627, Belo Horizonte - MG, 31270-901, Brazil
luizm@demec.ufmg.br, rphnunes@demec.ufmg.br

Abstract. *One way to reduce electricity consumption is to use heat pumps assisted by solar energy instead of electric heaters. Several studies were found using solar-assisted heat pumps that use either a thermostatic expansion valve or an electronic expansion valve, but there is a few work on solar-assisted heat pumps using capillary tubes despite the low cost of this device. In this work, an analysis of the technical and economic feasibility of using the capillary tube will be performed instead of thermostatic valves in heat pumps assisted by solar energy. In this analysis a lumped model will be used for each component of the system. This model was experimentally validated using a direct expansion heat pump assisted by solar energy (DX-SAHP) equipped with a thermostatic expansion valve. The performance of the heat pump will be compared using a thermostatic expansion valve and three capillary tubes for different values of ambient temperature and solar radiation. Finally, a case study will be carried out considering the climatic conditions and costs in the city of Belo Horizonte, comparing the Payback related to the replacement of electric heaters by heat pumps assisted by solar energy using capillary tubes and thermostatic valves.*

Keywords: *Capillary tube, Heat pump, Direct expansion, Solar energy*

1. INTRODUCTION

Solar energy has received a lot of attention in recent years due to the growing need for electricity globally. And a way to mitigate this consumption is the use of heat pumps assisted by solar energy (SAHP) to produce hot water, which is currently a constant demand of society, instead of using electrical resistance. What makes the heat pump more advantageous is its high thermal efficiency, as investigated by Chua *et al.* (2010).

Panaras *et al.* (2013), investigated the performance of a water heating system aided by a heat pump. The system has proven to achieve significant auxiliary energy savings compared to the integration of an electrical resistance or a direct burn heater. The results showed that the savings annually can reach 70% for the climatic data of the studied region.

Bengtsson and Berghel (2016) presented a study to reduce the electric energy consumption of a dishwasher. For this purpose, a heat pump for heating water was connected to the dishwasher, which has a capillary tube as an expansion device. The author evaluated the equipment with several masses of refrigerant fluid and different lengths of capillary tube. In the analysis, the lowest electricity consumption occurred with 60 g of refrigerant mass and 0.68 m in length of the capillary tube. Bengtsson *et al.* (2015) showed that there was a 24% reduction in electricity consumption with the use of a heat pump for water heating compared to traditional water heating systems.

In this paper, a technical and economical comparison is made between the solar assisted heat pump operated by a

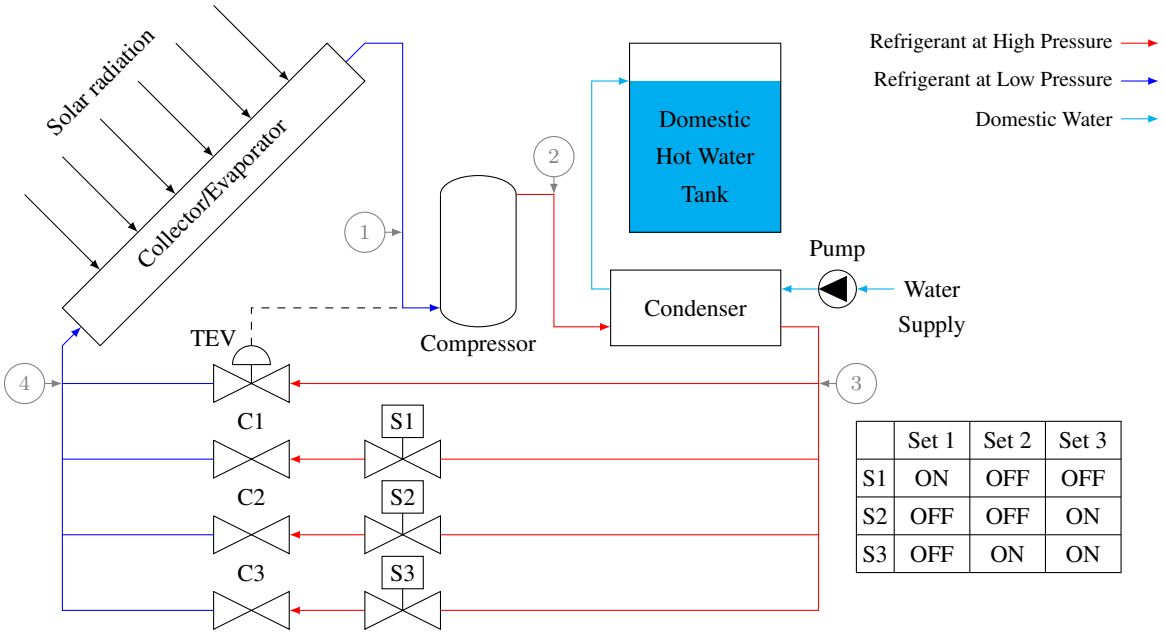

Figure 1. Direct expansion solar assisted Heat pump

thermostatic expansion valve with the same heat pump operated with three types of capillary tubes with three different configurations, as shown in Fig. 1. The ultimate goal is to evaluate the feasibility of developing a heat pump with a capillary tube expansion device.

2. MATHEMATICAL MODEL

The refrigerant chosen for this work is the R134a. R134a is more suitable for DX-SAHP than R410A, R407C and R404A (Chata *et al.*, 2005), it is the refrigerant most used in the recent studies of DX-SAHP (Kara *et al.*, 2008; Omojaro and Breitkopf, 2013; Mohanraj *et al.*, 2018a,b; Rabelo *et al.*, 2019) and, finally, it is the refrigerant used in the experimental tests used in the validation of the mathematical model (Diniz, 2017).

In order to evaluate the performance of DX-SAHP for producing DHW (domestic hot water) a quasi-steady-state model was developed using Equation Engineering Solver (EES). The losses in the tubes between components was considered negligible and for the inventory charge of the refrigerant, the pipeline was considered two meters long. The evaporator/solar collector and condenser was assumed as isobaric and a lumped model was used. Following is described the modeling equation for each component.

2.1 Compressor model

The refrigerant mass flow rate ($\dot{m}$) in a constant rotation speed reciprocating compressor is given by (Mohanraj *et al.*, 2018a):

$$\dot{m} = \rho_1 n V_s \eta_v \tag{1}$$

where ρ is the refrigerant density, n is the rotation speed (3500 rpm), V_s is the compressor swept volume (7,95cm^3/rev.), η_v is the volumetric efficiency and the subscript 1 refers to compressor inlet or evaporator outlet. The compressor electric power consumption ($\dot{W}$), considering a isentropic compression process, is evaluated as follow (Minetto, 2011):

$$\dot{W} = \frac{\dot{m}(i_{2S} - i_1)}{\eta_g} \tag{2}$$

where η_g is the global efficiency and i is the refrigerant specific enthalpy and the subscript $2S$ refers to compressor outlet considering an isentropic process. The global and volumetric efficiency was determinate fitting equations proposed by Minetto (2011) to the compressor performance map available in Embraco website. The global and volumetric efficiency is given by:

$$\eta_v = -0.0143 \left(\frac{P_2}{P_1}\right) + 0.915 \tag{3}$$

$$\eta_g = -0.0004 \left(\frac{P_2}{P_1}\right)^2 + 0.0104 \left(\frac{P_2}{P_1}\right) + 0.4839 \tag{4}$$

where P is the refrigerant pressure. The coefficient of determination (R^2) for volumetric efficiency is 97.6% and for global efficiency is 94.4%. In order to obtain with good precision the the discharge temperature of the compressor (T_2) an isentropic efficiency (η_i) of 85% was considered, and the entalphy at exit of the compressor evaluated as follow:

$$i_2 = \frac{i_{2S} - i_1}{\eta_i} + i_1 \tag{5}$$

2.2 Direct expansion solar evaporator

The heat transfer rate received by the refrigerant in the evaporator ($\dot{Q}_e$) is given by:

$$\dot{Q}_e = \dot{m}(i_1 - i_4) \tag{6}$$

where the subscript 4 refers to thermostatic valve outlet or evaporator inlet. To evaluate the energy gain in a flat plate collector in steady-state condition Kong *et al.* (2011) suggest the following equation:

$$\dot{Q}_e = A_e F'[S - U_L(\overline{T}_r - T_a)] \tag{7}$$

where A_e is the area of evaporator of the solar collector (1.65m^2), F' is the collector efficiency factor, S is the net radiation absolved per unit of area, U_L is overall heat loss coefficient, $\overline{T}_r$ is the average temperature of the refrigerant fluid and T_a is the ambient air temperature.

The collector effectiveness factor is calculated using the Hottel-Whilliar-Bliss model described by Duffie and Beckman (2013), considering that the resistance to heat flow due the bond between the collector plate and tube can be neglected, is given by:

$$F' = \frac{1}{U_{ev}} \left\{ W \left[\frac{1}{U_{ev}[D_o + F(W - D_o)]} + \frac{1}{\pi D_i h_i} \right] \right\}^{-1} \tag{8}$$

where the distance between the tubes in the evaporator is W, the fin efficiency is F, the outer diameter (8.73mm) is D_o, the inner diameter (9.53mm) is D_i, the internal convective coefficient is h_i that is calculated by the correlation proposed by Shah (2017) for two phase flow and by the correlation proposed by Gnielinski (1976) for single phase flow.

The fin efficiency can be evaluated by:

$$F = \frac{\tanh\left[(w - D_o)/2\sqrt{U_L/(k\delta)}\right]}{(w - D_o)/2\sqrt{U_L/(k\delta)}} \tag{9}$$

where δ is the fin thickness (1mm) and k is the thermal conductivity. The net radiation absolved is evaluated as made by Kong *et al.* (2017):

$$S = aI - \varepsilon\sigma(T_r^4 - T_s^4) \tag{10}$$

where the absorptivity is a, the solar radiation intensity normal to evaporator is I, the emissivity is ε, σ is the Stefane-Boltzmann constant and T_s is the sky temperature. The sky temperature was estimated by the method proposed by Gliah *et al.* (2011) using the correlation of Angstrom presented by Berdahl and Fromberg (1982) for sky emissivity (Eq. 11).

$$\varepsilon_{sky} = 0.734 + 0.0061 T_{dp} \tag{11}$$

The overall heat loss coefficient proposed by Kong *et al.* (2011) is determined by:

$$U_L = h_o + 4\varepsilon\sigma T_a^3 \tag{12}$$

where the external convective coefficient (h_o) is calculated by the collection of correlations for free and forced convection, depending on wind speed (u_w), for tilted flat plate listed by Neils and Klein (2009).

2.3 Coaxial condenser

During the operation with coaxial condenser, the hot water tank is filled with hot water, so the energy balance in the hot water tank is given by:

$$Q_t = \rho_w C_w \dot{\forall}_w (T_w - T_a) \tag{13}$$

The balance of energy in the refrigerant at the condenser is evaluated as follow:

$$Q_{cond} = \dot{m}_r(i_2 - i_3) \tag{14}$$

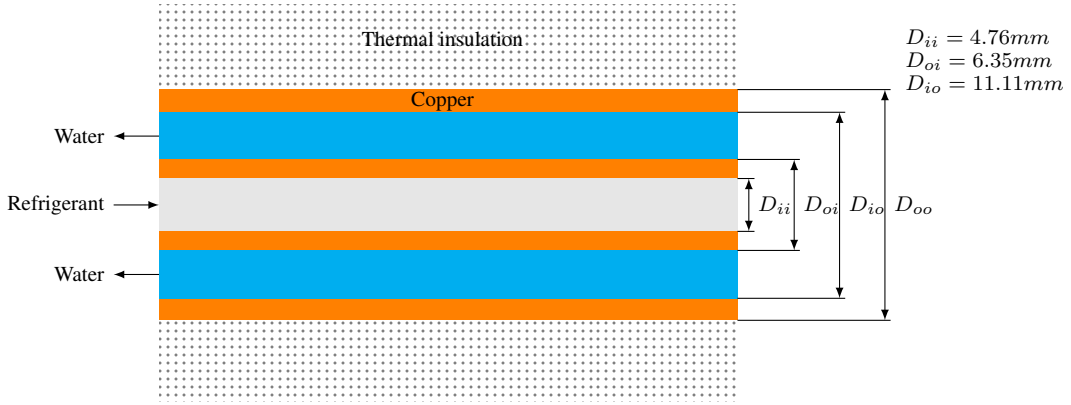

Figure 2. Concentric condenser geometric parameters

Assuming no heat loss in the coaxial condenser, the balance of energy in the water is given by:

$$Q_{cond} = \dot{m}_w C_w (T_{wo} - T_{wi}) \tag{15}$$

The heat transfer rate in the condenser is calculated using the effectiveness-NTU method. The effectiveness (ξ) of a concentric heat exchanger is evaluated as follows Incropera *et al.* (2007):

$$\xi = \frac{Q_{cond}}{\dot{C}_{min}(T_2 - T_{wi})} \tag{16}$$

$$\xi = \frac{1 - \exp[-\text{NTU}(1 - \dot{C}_{min}/\dot{C}_{max})]}{1 - \exp[-\text{NTU}(1 - \dot{C}_{min}/\dot{C}_{max})]\dot{C}_{min}/\dot{C}_{max}} \tag{17}$$

where $\dot{C}_{min}$ and $\dot{C}_{max}$ is the equal to $\dot{C}_r$ or $\dot{C}_w$, whichever is smaller and bigger, respectively. The refrigerant and water heat capacity rate are given by:

$$\dot{C}_r = \dot{m}_r \overline{C}_r \tag{18}$$

$$\dot{C}_w = \dot{m}_w C_w \tag{19}$$

In these equations, the mean specific heat of the refrigerant ($\overline{C}_r$) is evaluated by EQ. 20 and the Number of Transfer Units (NTU) by EQ. 21.

$$\overline{C}_r = \frac{i_2 - i_3}{T_2 - T_3} \tag{20}$$

$$\text{NTU} = \frac{UA}{\dot{m}_w C_w} \tag{21}$$

The UA value is determined by:

$$UA = \left(\frac{1}{\overline{h}_r \pi D_{ii} L_{cond}} + \frac{ln(D_{ii}/D_{io})}{2\pi k L_{cond}} + \frac{1}{\overline{h}_w \pi D_{oi} L_{cond}} \right)^{-1} \tag{22}$$

where the diameters D_{ii} and D_{oi} are shown in Fig. 2, L_{cond} is condenser length (5,5m), the mean water HTC ($\overline{h}_w$) is calculated using the correlations described by Duarte (2018) for flow in annular regions, and the mean refrigerant HTC ($\overline{h}_r$) is calculated assuming that the entalphy varies linearly with length and using the correlation of Gnielinski (1976) for h_r if $i \geq i_V$ or $i \leq i_L$ and the correlation of Shah (2016) if $i_L < i < i_V$.

In order to consider the heat loss at the water tank and in the connecting tubes before and after the condenser, Kong *et al.* (2011) propose a heat leakage coefficient of 95% given by:

$$\zeta = \frac{Q_t}{Q_{cond}} \tag{23}$$

2.4 Expansion device

In this study, three expansion device configurations were used, according to table 1, S1, S2 and S3. Capillary 1 diameter is 0.031 in a length of 3 m. Capillary 2 diameter is 0.064 in a length of 2.9 m. Capillary 3 diameter is 0.042 in a length of 1.25 m. As the settings are selected by the temperature sensor, which reads the superheat and sends the signal for opening and closing the solenoid valves.

To simulate the system operating with a capillary tube the mass flow ($\dot{m}$) is calculated using the correlation described by Rasti and Jeong (2018):

$$\dot{m} = 150,26\Pi_a^{-0,5708}\Pi_b^{-1,4636}\Pi_c^{1,953}\Pi_d^{0,6436}\Pi_e^{0,14181}\Pi_f^{-0,0158}D_c\mu_f \tag{24}$$

where L_{cap} is the capillary tube length, D_c is the capillary tube inside diameter, $P_{c,in}$ is the capillary tube inlet pressure, μ_f is the capillary inlet saturated liquid viscosity, ν_f is the capillary inlet liquid saturated specific volume, μ_f is the capillary inlet saturated vapor specific volume, i_{fgc} is the latent heat of vaporization at capillary inlet pressure, i_f is satured liquid specific enthalpy at capillary inlet pressure, $i_{c,in}$ is the capillary inlet specific enthalpy and L_{coil} is the coiled capillary tube length. Eq. 1 used to calculate the density at the inlet of the compressor, thence the superheating. The dimensionless parameters are shown in Tab. 1. The correlation of Rasti and Jeong (2018) yields good agreement with 1052 sets of experimental data produced from five different refrigerants, including the R134a.

Table 1. Dimensionless Parameters

Parameter	Definition	Description
Π_a	L_{cap}/D_c	Effect of capillary tube total length and inside diamenter
Π_b	$D_c^2 i_{fgc}/\nu_f^2\mu_f^2$	Effect of the latent heat of vaporization
Π_c	$D_c^2 P_{c,in}/\nu_f\mu_f^2$	Effect of the capillary tube inlet pressure
Π_d	$1+(i_{c,in}-i_f)/i_{fg}$	Effect of enthalpy at the capillary tube inlet
Π_e	ν_g/ν_f	Effect of the density
Π_f	$1+L_{coil}/d_{coil}$	Effect of the coiled capillary tube length and coil diameter

2.5 Refrigerant charge

Kong *et al.* (2017) and Zhang *et al.* (2014) showed that another important parameter is the refrigerant charge of DX-SAHP. The required mass of the refrigerant (m) is evaluated by the Eq. 25 for single phase flow and by the Eq. 26 for two phase flow.

$$m = \int \rho dV \tag{25}$$

$$m = \int \left[\alpha\rho_v + (1-\alpha)\rho_l\right] dV \tag{26}$$

where the subscripts l and v refers to the liquid and to the vapor, respectively, and the void fraction (α) is calculated by Hughmark (1965) correlation.

3. PERFORMANCE INDICATORS

The coefficient of performance (COP) and the solar collector efficiency (η_{col}) proposed by Kong *et al.* (2011, 2017) and Kuang *et al.* (2003) is defined as follow:

$$COP = \frac{\zeta \cdot \dot{Q}_{cond}}{\dot{W}} \tag{27}$$

$$\eta_{col} = \frac{\dot{Q}_e}{A_e I} \tag{28}$$

The payback period ($\hat{P}$) of the DX-SAHP over an capillary tube, in years, if ($\hat{P}$) is higher than one year is given by:

$$\hat{P} = \frac{\hat{I}}{\hat{S}(1+\text{IR})^{(\hat{P}-1)}} \tag{29}$$

Table 2. Simulation parameters list

Parameter	Value	Parameter	Value	Parameter	Value
Heating demand	350 days/year	Inflation rate	10%	Initial water temperature	25 ^{o}C
Atmospheric Pressure	101.3 kPa	Collector tilt angle	30 ^{o}	Final water temperature	45 ^{o}C
Emissivity	0.95	Solar absorptivity	0.95	Ambient temperature	25 ^{o}C
Solar radiation	700 W/m^2	Superheating	7.4 ^{o}C	Subcooling	6.5^{o}C
Initial Investment with capillary	4550BRL	Mass of R134a	0,29kg	Electricity tariff	0.95 BRL/kWh
Initial Investment with TEV	4400BRL	Water tank size	0.2 m^3	Capillary coil diameter	5 cm

where $\hat{I}$ is the difference of initial investment between DX-SAHP and an capillary tube, IR is the annual inflation rate and the annual savings ($\hat{S}$). The mean inflation rate of electricity in Brazil is 10% (Santos *et al.*, 2018). The annual savings that is given by:

$$\hat{S} = Q_A \left(\frac{\hat{E}}{\eta_e} - \frac{\hat{E}}{COP} \right) \tag{30}$$

where $\hat{E}$ is the electricity tariff, Q_A is annual heat demand and η_e is the efficiency of electrical heater (97%).

In order to compare the accuracy of the model, the most used metrics are the Mean Absolute Deviation (MAD) and Mean Deviation (MD). For COP the MAD and MD are evaluated as showed in EQ. 31 and 32. The compressor outlet temperature (T_2) is calculated in similar way.

$$\text{MAD} = \frac{1}{n} \sum_{j=1}^{n} \left| \frac{COP_{calc} - COP_{exp}}{COP_{exp}} \right| \tag{31}$$

$$\text{MD} = \frac{1}{n} \sum_{j=1}^{n} \left(\frac{COP_{calc} - COP_{exp}}{COP_{exp}} \right) \tag{32}$$

A list of the parameters used in the following simulations is presented in Tab. 2. The costs in Tab. 2 are based in the Belo Horizonte market in March of 2020. The subcooling in Tab. 2 is used only for simulation with a thermostatic expansion valve and the refrigerant charge in the simulation with capillary tube.

4. RESULTS

4.1 Model validation

The model validation is performed comparing the experimental results using a TEV presented by Diniz (2017) combined by the data available in Brazilian National Institute of Meteorology (INMET) web site. The comparison between measured and calculated COP and outlet compressor temperature is shown in the Tab. 3. The subcooling was assumed fixed in 6.5^{o}C, which represents the average value in the experimental tests. In table 3, the uncertainty of the water inlet temperature (T_{wi}), water outlet temperature T_{wo} and ambient temperature (T_a) is $\pm 1^o$C, for dew point temperature (T_{dp}) is $\pm 2^o$C, for the superheating at exit of evaporator (ΔT_{sh}) is $\pm 1.4^o$C, for the atmospheric pressure $\pm$2kPa, for the solar radiation (I) is $\pm$5% and for wind speed (u_w) is $\pm$3%. The experimental results present good accuracy, 5.2% of uncertainty for COP and 1.4% for discharge temperature.

Table 3. Results of experimental modeling validation

Test	Date	T_a	P_{atm}	T_{dp}	I	u_w	T_{wi}	T_{wo}	ΔT_{sh}	T_2		COP	
	dd/mm/yy	^{o}C	kPa	^{o}C	W/m^2	m/s	^{o}C	^{o}C	^{o}C	Exp.	Calc.	Exp.	Calc.
1	12/01/17	27.1	91.5	17.2	0	0	27.3	44.8	7.1	71.1±1.0	63.8±1.1	2.37±0.12	2.19±0.03
2	13/01/17	26.6	91.5	20.2	0	0	26.3	45.3	7.1	72.0±1.0	63.4±1.1	2.25±0.12	2.20±0.03
3	16/01/17	24.9	91.7	19.4	0	0	25.0	46.0	7.1	72.2±1.0	62.7±1.1	2.26±0.11	2.20±0.03
4	17/01/17	26.1	91.5	17.2	0	0	25.1	46.0	7.1	72.6±1.0	62.9±1.1	2.36±0.12	2.20±0.03
5	19/01/17	26.5	91.7	18.4	0	0	25.8	45.5	7.1	72.1±1.0	63.1±1.1	2.32±0.12	2.20±0.03
6	23/01/17	29.7	91.9	15.6	421	0.52	27.6	46.7	7.8	73.2±1.0	70.8±1.1	2.56±0.13	2.47±0.04
7	25/01/17	32.9	92.0	16.3	709	0.86	28.7	47.4	7.8	74.7±1.0	76.8±1.1	2.72±0.14	2.62±0.04
8	25/01/17	32.7	92.0	16.6	758	0.95	29.3	47.3	7.8	75.4±1.0	77.8±1.1	2.64±0.14	2.63±0.04
9	27/01/17	32.5	92.1	13.5	629	1.16	29.0	45.9	7.8	73.9±1.0	74.9±1.2	2.69±0.14	2.60±0.05
10	28/01/17	31.2	92.1	13.3	811	1.36	29.0	47.8	7.8	73.7±1.0	78.2±1.2	2.48±0.13	2.64±0.04

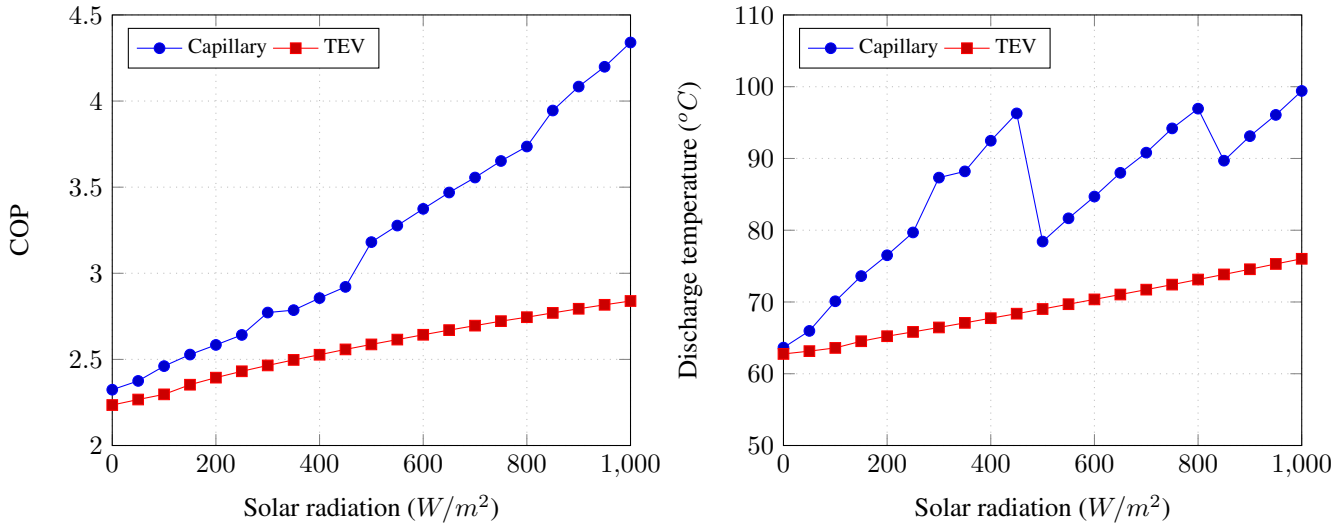

Figure 3. Variation of COP and outlet compressor temperature with solar radiation

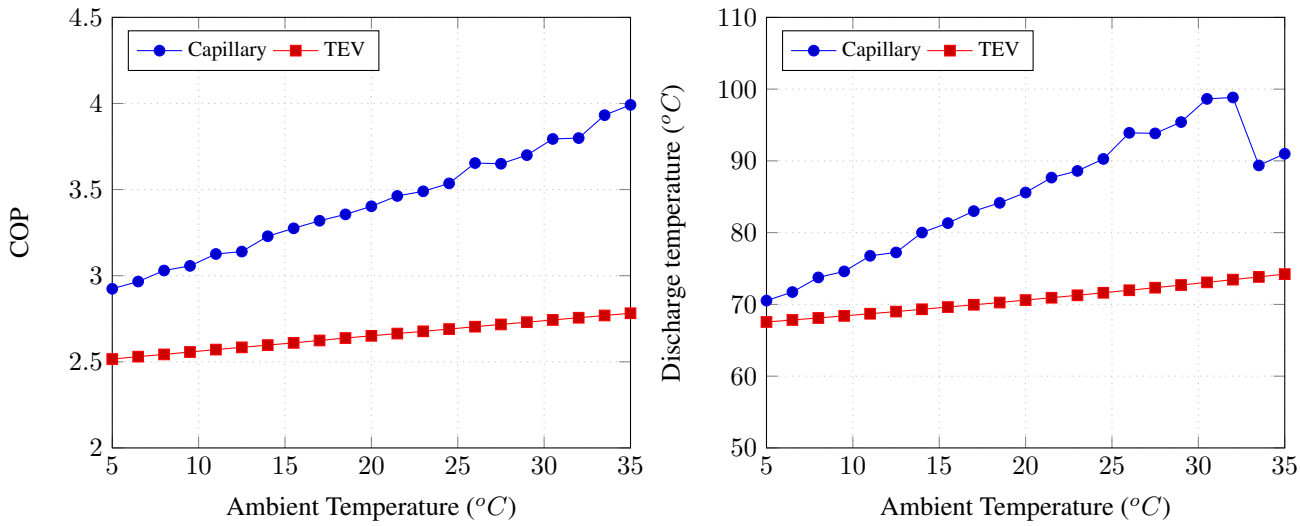

Figure 4. Variation of COP and outlet compressor temperature with ambient temperature

The MAD and MD of COP are respectively 4.2±4.8% and 2.9±5.2%. Considering the uncertainty range, there is no mean difference of experimental COP and calculated COP. The MAD and MD of compressor outlet temperature are respectively 7.8±2.0% and 5.1±2.0%. The MAD and MD of compressor outlet temperature considering only the tests 6 to 10 are respectively 3.3±2.0% and -2.0±2.0%. Considering the uncertainty range and the experimental test with solar radiation, the most import for this work, there is no mean difference of experimental discharge temperature and calculated discharge temperature. For COP, the uncertainty of the model was four time lower than than that obtained experimentally. For discharge temperature, the uncertainty of the model was higher than that obtained experimentally.

4.2 Energetic and economical performance

The COP and outlet compressor temperature for different solar radiation and ambient temperature are showed in Fig. 3. The discontinuity around 475W/m^2 and 825W/m^2 is due the change of the set of solenoids. The set of solenoids are chose to keep the compressor outlet temperature lower than 100^{o}C. The COP and discharge temperature of the system at 700W/m^2 using the capillary is 32% and 27% higher than COP and discharge temperature using a TEV. The difference in the COP is justified due the higher evaporation pressure (17%) and lower condensation pressure (31%) when the system with capillary is used. The difference in the discharge temperature is justified due the superheat, 43.8^{o}C in this case.

In Fig. 3 and Fig. 4, it is clearly seen that the COP increases with the increase of solar radiation intensity and ambient temperature, this is mainly because the increase radiation and ambient temperature enables to attain a higher evaporating

temperature of the refrigerant, consequently resulting in a higher COP. For 700W/m^2 the COP for the capillary tube is 39% higher than TEV.

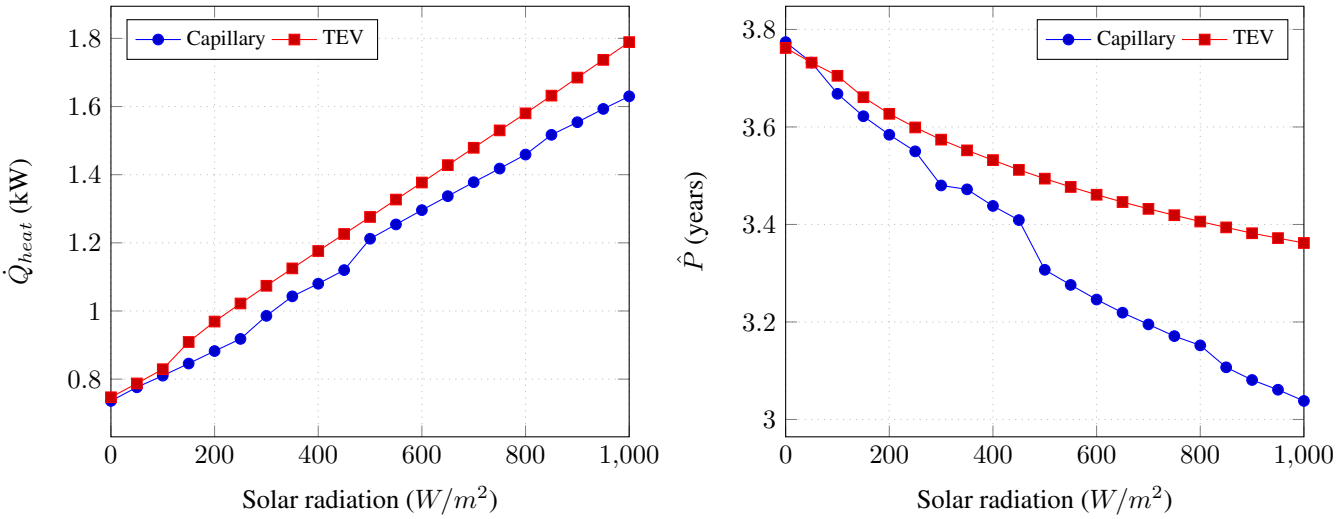

Figure 5. Variation of Payback and heat capacity with solar radiation

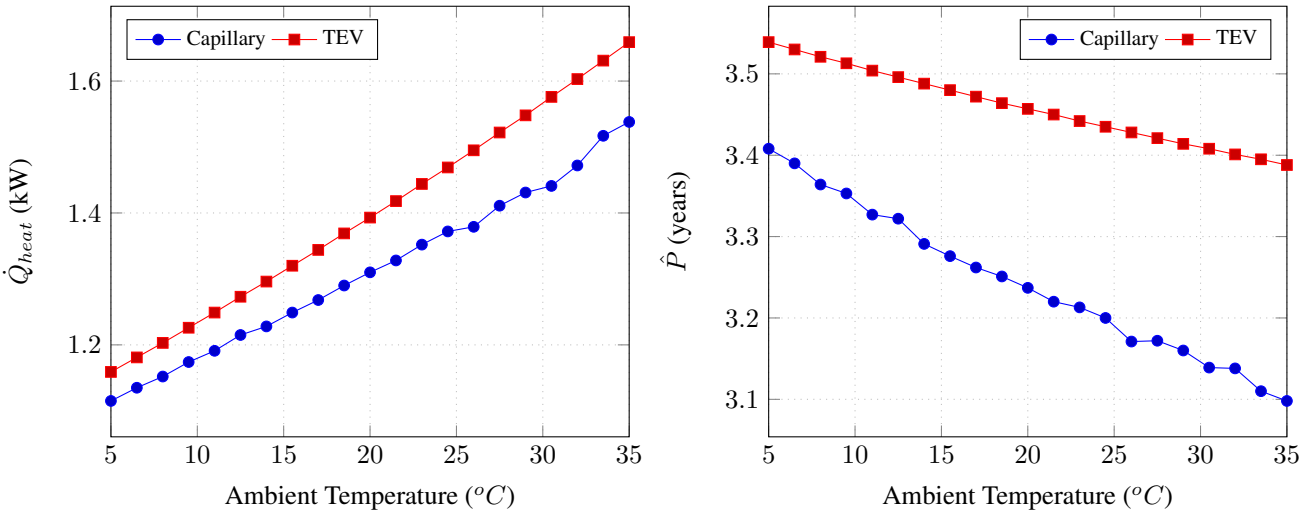

Figure 6. Variation of Payback and heat capacity with ambient temperature

The initial investment for the capillary tube is greater, as shown in table 2, due to the high cost of the solenoid valves, but the payback period, shown in Fig. 5, is shorter for capillary tubes, approximately 8% lower for 700W/m^2 and water heating capacity is slightly lower for the capillary tube due to the lower flow of water in the condenser, around 7% less than the TEV. For greater ambient temperature, as shown in Fig. 6, the payback period is shorter and the heating capacity is greater. The operation time of the DX-SAHP, as shown in Fig. 7, is approximately 3.5 hours for both expansion devices.

5. CONCLUSION

In this work a mathematical model DX-SAHP for producing domestic hot water is used to compare the performance of the heat pump using a thermostatic expansion valve between a heat pump using three capillary tubes as expansion device, evaluated for different values of ambient temperature and solar radiation. The results showed that the COP and discharge temperature using capillary tube, for average solar radiation of 700W/m^2, is 32% and 27% higher than using a TEV. The initial investment with TEV is lower but payback period is less for the capillary tube. Finally, considering that it is not easy to find small capacity VET for refrigerant R290, three capillary tubes become viable for application in solar assisted heat pumps.

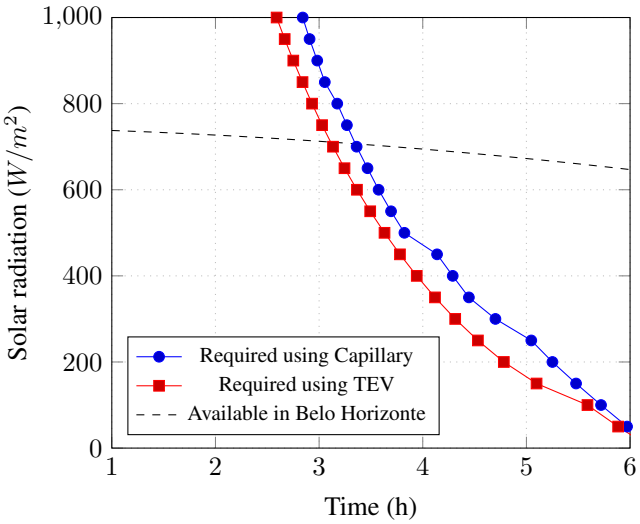

Figure 7. Required and available solar radiation in function of time of operation

6. ACKNOWLEDGEMENTS

This work was supported by Foundation for Research Support of the State of Minas Gerais (FAPEMIG), National Council for Scientific and Technological Development (CNPq) and Coordination of Improvement of Higher Level Personnel (CAPES).

7. REFERENCES

Bengtsson, P. and Berghel, J., 2016. "Study of using a capillary tube in a heat pump dishwasher with transient heating". *International Journal of Refrigeration*, Vol. 67, pp. 1– 9.

Bengtsson, P., Berghel, J. and Renstrom, R., 2015. "A household dishwasher heated by a heat pump system using an energy storage unit with water as the heat source". *International Journal of Refrigeration*, Vol. 49, pp. 19– 27.

Berdahl, P. and Fromberg, R., 1982. "The thermal radiance of clear skies". *Solar Energy*, Vol. 29, No. 4, pp. 299 – 314.

Chata, F.G., Chaturvedi, S. and Almogbel, A., 2005. "Analysis of a direct expansion solar assisted heat pump using different refrigerants". *Energy Conversion and Management*, Vol. 46, No. 15, pp. 2614–2624.

Chua, K., Chou, S. and Yang, W., 2010. "Advances in heat pump systems: A reveiw". *Applied Energy*, Vol. 87, pp. S3611–S3624.

Diniz, H.A.G., 2017. *Estudo comparativo da eficiência energética de uma bomba de calor assistida por energia solar operando com condensadores por imersão e coaxial*. Master's thesis, UFMG, Belo Horizonte, MG, Brazil.

Duarte, W.M., 2018. *Numeric model of a direct expansion solar assisted heat pump water heater operating with low GWP refrigerants (R1234yf, R290, R600a and R744) for replacement of R134a*. Ph.D. thesis, UFMG.

Duffie, J.A. and Beckman, W.A., 2013. *Solar engineering of thermal processes*. John Wiley & Sons.

Gliah, O., Kruczek, B., Etemad, S.G. and Thibault, J., 2011. "The effective sky temperature: an enigmatic concept". *Heat and mass transfer*, Vol. 47, No. 9, pp. 1171–1180.

Gnielinski, V., 1976. "New equations for heat and mass transfer in turbulent pipe and channel flow". *Int. Chem. Eng.*, Vol. 16, No. 2, pp. 359–368.

Hughmark, G., 1965. "Holdup and heat transfer in horizontal slug gas-liquid flow". *Chemical Engineering Science*, Vol. 20, No. 12, pp. 1007–1010.

Incropera, F.P., Lavine, A.S., Bergman, T.L. and DeWitt, D.P., 2007. *Fundamentos da Transferência do Calor e massa*. Editora LTC, 6th edition.

Kara, O., Ulgen, K. and Hepbasli, A., 2008. "Exergetic assessment of direct-expansion solar-assisted heat pump systems: review and modeling". *Renewable and Sustainable Energy Reviews*, Vol. 12, No. 5, pp. 1383–1401.

Kong, X., Li, Y., Lin, L. and Yang, Y., 2017. "Modeling evaluation of a direct-expansion solar-assisted heat pump water heater using R410A". *International Journal of Refrigeration*, Vol. 76, pp. 136–146.

Kong, X., Zhang, D., Li, Y. and Yang, Q., 2011. "Thermal performance analysis of a direct-expansion solar-assisted heat pump water heater". *Energy*, Vol. 36, No. 12, pp. 6830–6838.

Kuang, Y., Sumathy, K. and Wang, R., 2003. "Study on a direct-expansion solar-assisted heat pump water heating system". *International Journal of Energy Research*, Vol. 27, No. 5, pp. 531–548.

Minetto, S., 2011. "Theoretical and experimental analysis of a CO_2 heat pump for domestic hot water". *International*

journal of refrigeration, Vol. 34, No. 3, pp. 742–751.

Mohanraj, M., Belyayev, Y., Jayaraj, S. and Kaltayev, A., 2018a. "Research and developments on solar assisted compression heat pump systems – A comprehensive review (Part A: Modeling and modifications)". *Renewable and Sustainable Energy Reviews*, Vol. 83, pp. 90 – 123. ISSN 1364-0321.

Mohanraj, M., Belyayev, Y., Jayaraj, S. and Kaltayev, A., 2018b. "Research and developments on solar assisted compression heat pump systems – A comprehensive review (Part-B: Applications)". *Renewable and Sustainable Energy Reviews*, Vol. 83, pp. 124 – 155.

Neils, G. and Klein, S., 2009. *Heat Transfer*. Cambridge university press.

Omojaro, P. and Breitkopf, C., 2013. "Direct expansion solar assisted heat pumps: A review of applications and recent research". *Renewable and Sustainable Energy Reviews*, Vol. 22, pp. 33 – 45. ISSN 1364-0321.

Panaras, G., Mathioulakis, E. and Belessiotis", V., 2013. "Investigation of the performance of a combined solar thermal heat pump hot water system". *Solar Energy*, Vol. 93, pp. 169 – 182.

Rabelo, S.N., Paulino, T.F., Machado, L. and Duarte, W.M., 2019. "Economic analysis and design optimization of a direct expansion solar assisted heat pump". *Solar Energy*, Vol. 188, pp. 164 – 174. ISSN 0038-092X.

Rasti, M. and Jeong, J.H., 2018. "A generalized continuous empirical correlation for the refrigerant mass flow rate through adiabatic straight and helically coiled capillary tube". *Applied thermal Engineering*, Vol. Final Report, No. 450-460, p. 11.

Santos, J.O., Cataldi, M., Herzog, M.M. and Pereira, E.M.D., 2018. "Comparação econômica entre o sistema de refrigeração fotovoltaico por compressão de vapor e chillers de absorção com coletores solares térmicos". In *CBENS 2018: VII Congresso Brasileiro de Energia Solar*. ABENS.

Shah, M.M., 2016. "Comprehensive correlations for heat transfer during condensation in conventional and mini/micro channels in all orientations". *International journal of refrigeration*, Vol. 67, pp. 22–41.

Shah, M.M., 2017. "Unified correlation for heat transfer during boiling in plain mini/micro and conventional channels". *International Journal of Refrigeration*, Vol. 74, pp. 604–624.

Zhang, D., Wu, Q., Li, J. and Kong, X., 2014. "Effects of refrigerant charge and structural parameters on the performance of a direct-expansion solar-assisted heat pump system". *Applied Thermal Engineering*, Vol. 73, No. 1, pp. 522 – 528.

8. RESPONSIBILITY NOTICE

The authors are the only responsible for the printed material included in this paper.